JOURNAL OF VIROLOGY, Aug. 1991, p. 4153–4159
0022-538X/91/084153-07$02.00/0

Vol. 65, No. 8

# Generation and Analysis of Nonhomologous RNA-RNA Recombinants in Brome Mosaic Virus: Sequence Complementarities at Crossover Sites

JOZEF J. BUJARSKI* AND ALEKSANDRA M. DZIANOTT

*Plant Molecular Biology Center and Department of Biological Sciences, Northern Illinois University, DeKalb, Illinois 60115-2861*

Received 8 January 1991/Accepted 20 April 1991

**All three single-stranded RNAs of the brome mosaic virus (BMV) genome contain a highly conserved, 193-base 3′ noncoding region. To study the recombination between individual BMV RNA components, barley plants were infected with a mixture of in vitro-transcribed wild-type BMV RNAs 1 and 2 and an RNA3 mutant that carried a deletion near the 3′ end. This generated a population of both homologous and nonhomologous 3′ recombinant BMV RNA3 variants. Sequencing revealed that these recombinants were derived by either single or double crossovers with BMV RNA1 or RNA2. The primary sequences at recombinant junctions did not show any similarity. However, they could be aligned to form double-stranded heteroduplexes. This suggested that local hybridizations among BMV RNAs may support intermolecular exchanges.**

As in DNA-based organisms, genetic recombination in RNA viruses provides a means for their well-known rapid evolution and adaptation (20, 34). Natural RNA rearrangements have been identified in the genomes of several plant RNA virus groups, including beet necrotic yellow vein virus (7), tombusviruses (15), tobamoviruses (33), and tobraviruses (30). In addition, the recombination has been induced experimentally. For example, a temperature-sensitive mutation in the RNA3 component of alfalfa mosaic virus acquired a 5′-terminal fragment from the RNA1 component during infection (16). An insertion mutant of tobacco mosaic virus easily lost one of its duplicate coat protein cistrons (12). Cascone et al. have detected a recombination between the satellite and defective interfering RNAs of turnip crinkle virus (TCV) (11).

One of the most useful experimental systems with which to study recombination in plant viruses is bromoviruses. Brome mosaic virus (BMV) is a tripartite positive-stranded RNA virus whose RNA components share a highly structured 3′ noncoding region of nearly 200 nucleotides (2). Previously, Bujarski and Kaesberg (10) found that a biologically active deletion mutant of BMV RNA3 (designated M4; Fig. 1) was efficiently repaired by recombination between M4 and the noncoding sequences of wild-type (wt) RNA1 or RNA2, in either homologous or nonhomologous fashions. Rao et al. (28) confirmed these results by studying the recombinational repair of 3′ deletion mutations in BMV RNA2. In cowpea chlorotic mottle virus, another bromovirus, Allison et al. (3) have demonstrated the regeneration of a functional RNA3 molecule by recombination between two overlapping internal deletion mutants. Because the majority of all these identified bromovirus recombinants were homologous, the sequences at crossover sites were unrecognizable. This seriously limited our understanding of the recombination mechanism in these viruses.

Many more data about RNA-RNA recombination are available for animal RNA viruses, especially picornaviruses and coronaviruses (19, 21, 25). Kirkegaard and Baltimore have demonstrated that intertypic homologous recombination between two poliovirus types occurred via a copy choice mechanism during negative-strand synthesis (22). Other studies implied that certain RNA structures may facilitate recombination crossings. For instance, both Kirkegaard and Baltimore (22) and Tolskaya et al. (35) found that crossovers among poliovirus types were restricted to certain virus RNA segments. The latter group found that these RNA segments had the potential to form secondary structures (31). Based on this observation, the authors suggested that the formation of intermolecular duplexes induced the intermolecular replicase switches. In a modification of this model, Kuge et al. (23) proposed that poliovirus defective interfering RNAs were generated by a looping-out process at the two RNA sites that have been juxtaposed by another complementary RNA molecule. In coronaviruses, recombinational exchanges were also limited to selected RNA locations (5).

In an attempt to advance our insight into the mechanism of RNA recombination in plant viruses, we characterized a number of nonhomologous BMV RNA3 recombinants that were obtained after infection with the M4 RNA3 mutant. A comparison of sequences at the nonhomologous junctions has shown that the crossovers took place within the potential double-stranded regions. This inferred that, as in poliovirus, local hybridizations can provide an environment for the RNA exchanges.

## MATERIALS AND METHODS

**Materials.** Plasmids pB1TP3, pB2TP5, and pB3TP7 (a generous gift from Paul Ahlquist, University of Wisconsin, Madison), containing full-length cDNA copies of wt BMV RNA components 1, 2, and 3, were used to synthesize infectious BMV transcripts. A previously constructed derivative of pB3TP7 (8) was used to synthesize the M4 RNA3 transcript (Fig. 1).

Avian myeloblastosis virus (AMV) reverse transcriptase was obtained from Life Sciences, Inc., St. Petersburg, Fla.; the Sequenase kit was from United States Biochemicals, Cleveland, Ohio; restriction enzymes were from Bethesda

* Corresponding author.

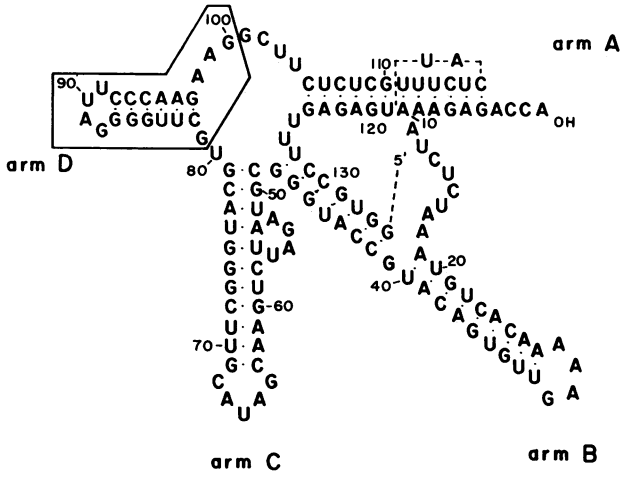


FIG. 1. Schematic representation of the tRNA-like conformation formed at the 3'-terminal noncoding region in BMV RNA3 according to Rietveld et al. (29). The location of the 20-nucleotide deletion (deletion M4) is indicated by an open box. The construction of the M4 BMV RNA3 deletion mutant was described previously (8).

Research Laboratories, Gaithersburg, Md.; T7 RNA polymerase was from Promega Corp., Madison, Wis. All radioactive chemicals were from Amersham Corp., Arlington Heights, Ill. Deoxyoligonucleotides were synthesized in an Applied Biochemicals DNA synthesizer at Northern Illinois University.

**Generation of BMV variants containing RNA3 recombinant molecules.** The wt BMV RNAs 1 and 2 as well as the M4 RNA3 were synthesized separately by transcription from 4 μg of the corresponding *Eco*RI-linearized plasmids by using T7 RNA polymerase, as described elsewhere (18). A mixture of the above transcripts was inoculated on eight 5-day barley seedlings, exactly as described by Allison et al. (3). Ten days following inoculation, the progeny viral RNAs were extracted from 0.2 g of infected leaves (24) and analyzed electrophoretically in 1% agarose gels with Tris-borate buffer (32). The progeny virus, isolated from one BMV-infected barley plant that contained the heterogeneous RNA3 component, was mechanically reinoculated on eight new barley seedlings, and the virus was extracted separately from 0.2 g of each plant 10 days after inoculation. After isolation from virions, each RNA preparation was analyzed electrophoretically in 1% agarose gels and subsequently used as the template to obtain cDNA libraries.

**Generation of cDNA libraries.** cDNA libraries for recombinant RNA3 molecules were obtained by a modification of the procedure described by Bujarski and Kaesberg (10). BMV RNA (20 μg) was hybridized to 1 μg of the deoxyoligonucleotide d(TGGTCTCTTTTAGAGA), which was complementary to the last 16 nucleotides of three BMV RNAs. Subsequently, this primer was extended with AMV reverse transcriptase as described elsewhere (14). The RNA strand was removed by RNase A digestion, and the resulting single-stranded (ss) cDNA was purified on a Sephadex G50 (Pharmacia) column (0.3 by 2 cm) in TE buffer (32). Then, 100 ng of the RNA3-specific second-strand synthesis primer [a 20-mer, d(GTTGTACATCTAGAAGTTGA), complementary between nucleotides 1752 and 1771 of the wt RNA3] was hybridized to the ss cDNA in a 20-μl mixture containing 10 mM Tris (pH 7.5), 10 mM $MgCl_2$, and 50 mM NaCl by incubation at 100°C for 3 min and then a graduate decrease to room temperature over 40 min. Subsequently, 0.5 mM each of four deoxynucleoside triphosphates and 3 mM dithiothreitol (final concentrations) were added, and the resulting mixture was incubated with 10 U of Klenow DNA polymerase at room temperature for 2 h in a final volume of 30 μl. The resulting double-stranded cDNA product was digested at the *Xba*I restriction site (present within the 20-mer primer) and ligated between the *Sma*I and *Xba*I restriction sites of the pGEM3-zf(+) cloning vector (Promega Corp.).

**Selection and sequencing of cDNA clones.** Approximately 1 μg of minilysate DNA preparations (32) of each cDNA library was digested with *Eco*RI and *Xba*I restriction enzymes, and the size of inserted cDNA fragments was estimated electrophoretically in 1% agarose gels. Thirty insert-containing clones from each library were sequenced with the Sequenase kit according to the manufacturer's specifications, initially with a single-nucleotide reaction ("A" track), and thereafter, those with different patterns were sequenced completely.

**Computer-assisted analysis of RNA sequences.** Sequences were aligned and folded by using the programs BESTFIT, FOLD, and GAP of the University of Wisconsin Genetics Computer Group sequence analysis package.

## RESULTS

**Derivation of nonhomologous RNA3 recombinants.** In order to generate nonhomologous RNA3 recombinants, eight barley seedlings were inoculated with the mixture of wt RNAs 1 and 2 and the M4 RNA3. This caused infection in three plants. The low infectivity (compared with the infectivity of the wt BMV RNA transcripts [18]) was probably caused by increased instability of the M4 RNA3 mutant or by alteration

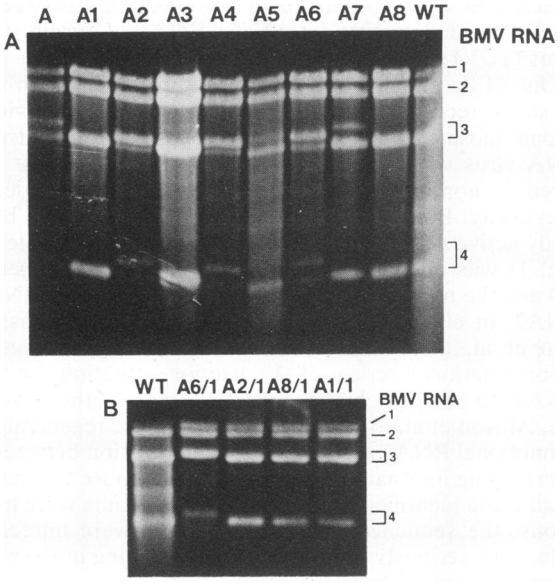


FIG. 2. Electrophoretic analysis (in 1% agarose gel) of progeny virion RNA isolated from BMV-infected barley leaves. (A) BMV RNAs extracted from initially inoculated plant A (lane A) and after first passage (lanes A1 to A8). (B) BMV RNAs isolated after second passage from plants A1/1, A2/1, A6/1, and A8/1. The missing RNA1 band in the wt lane is probably due to degradation during electrophoresis.

TABLE 1. Distribution of RNA3 recombinants in BMV-infected barley plants[a]

| Recombinant | Recombinant content (%) in plant: | | | | | | | |
|---|---|---|---|---|---|---|---|---|
| | A | A1 | A2 | A3 | A4 | A5 | A6 | A7 |
| 1 | 19.8 | | | | | | | 6.6 |
| 1′ | 3.3 | | | | | | | |
| 2 | 3.3 | | | | 83.4 | | 6.6 | |
| 3 | | | | | | | 73.6 | |
| 4 | 10.0 | | 83.5 | | | 56.1 | | |
| 5 | | | | | 6.6 | | | |
| 6 | | | | 6.6 | | | | |
| 7 | 10.0 | | | | | 43.9 | 19.8 | 90.1 |
| 8 | 33.8 | 96.7 | | 86.8 | 10.0 | | | |
| 9 | 19.8 | 3.3 | 16.5 | 6.6 | | | | 3.3 |

[a] The table shows the percentage of various RNA3 recombinants found in cDNA libraries obtained for the progeny BMV RNA extracted from primarily inoculated plant A and from seven plants (A1 to A7) infected with the virus inoculum from plant A. Plant A8 has not been analyzed. See Fig. 2 for the plant names. The percentage was calculated after the sequencing of 30 clones from each cDNA library (see Materials and Methods), i.e., one clone corresponds to 3.3%. The structures of recombinants 1 to 8 are shown in Fig. 4. Variant 9 represents the unrepaired M4 RNA3.

of the interactions with some virus and/or host factor. While progeny BMV RNA3 from two plants comigrated electrophoretically with the wt BMV RNA3 (data not shown), the one from a third plant (designated plant A) revealed two major bands at the region of RNA3 (lane A in Fig. 2A). This suggested that an extensively altered RNA component was present in the progeny virus.

To induce higher diversity among the RNA3 molecules, the virus isolated from plant A was reinoculated on eight new barley seedlings. An electrophoretic analysis (Fig. 2A, lanes A1 to A8) revealed that for three plants (lanes A1, A3, and A8), only one band was present at the RNA3 region, whereas in plants A2 and A4, two bands were visible in this area. The concentration of upper bands was higher than with the wt. In two other plants (A5 and A6), RNA3 was also composed of two bands, but the higher bands contained slightly larger RNA than those of plants A2 and A4. The RNA from plant A7 looked similar to that from plant A, but the upper RNA3 band was less intense. All this suggested a rapid generation of the illegitimate RNA3 molecules.

To examine whether the RNA3 profiles would undergo further changes, the viruses obtained after the first reinoculation were passaged on the new barley plants. As shown in Fig. 2B, double bands present in the region of RNA3 migration in plants A2 and A6 were replaced by single bands in plants A2/1 and A6/1. While in plant A2/1, the RNA3 entity comigrated with the wt RNA3, in plant A6/1, the more slowly migrating RNA3 band became predominant. The wt RNA3 profiles of plants A1 and A8 were retained in plants A1/1 and A8/1.

The heterogeneity of RNA4 populations in plants A2, A4, and A6 corresponded to that of RNA3 (Fig. 2A). In plants A, A5, and A7, however, only one band of RNA4 could be found, while two bands were observed in the region of RNA3. This might be because plants A, A5, and A7 contain larger RNA3 versions than plants A2, A4, and A6, rendering the corresponding RNA4 versions too big to be copackaged with the RNA3 components in the icosahedral virions. Alternatively, certain recombinant RNA3 molecules may have failed to serve as templates to generate subgenomic RNA4.

The predominance of the illegitimate variants, like that in plant A6/1, was surprising, especially since the wt-like (legitimate) recombinants were available for selection in the originally infected plant A (Table 1). All the prevalent illegitimate recombinants carried an unmodified 3′ tRNA-like structure (Fig. 3), the region known to serve as the replication promoter (1, 26). Therefore, one may speculate that they replicated with a rate similar to that of the wt-like recombinants and thus both types had comparable chances for selection.

Collectively, these results demonstrated that both legitimate and illegitimate BMV RNA variants readily emerged after infection. Most of the recombinants appeared in the originally inoculated plant A (Table 1), and subsequent passages caused further selection rather than generating new recombinants. This indicated that the M4 RNA3 was less genetically stable than the progeny illegitimate recombinants. One feature that may function against the endurance of the M4 mutant in infection is its higher-than-wt replication rate (8). This may disturb the appropriate balance between BMV RNA components in infection.

**Cloning and sequencing of recombinants.** To characterize the recombinant RNA3 molecules, 30 cDNA clones were

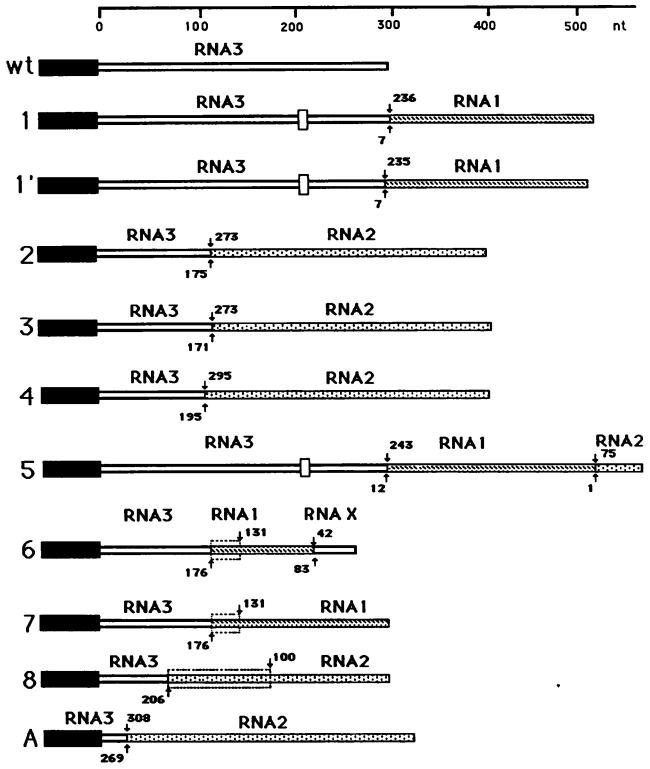


FIG. 3. Schematic representation of the BMV RNA3 recombinants (numbered 1 to 8) found in the infected barley plants (see Table 1). The figure shows the 3′ noncoding region of BMV RNA3 downstream of the coat protein cistron (solid box on the left), with the original RNA3 sequences shown as open boxes and acquired RNA1 or RNA2 sequences shown as cross-hatched boxes. The position of the unrepaired M4 deletion is shown by a small vertical rectangular open box. The location of each recombinant junction is identified by the sequence coordinates, numbered from the 3′ end. The regions where homologous recombination events occurred are enclosed in dotted open boxes. RNA X in the recombinant 6 line indicates that, due to sequence identity, the 3′-terminal region can be derived by crossings between any of the BMV RNAs.

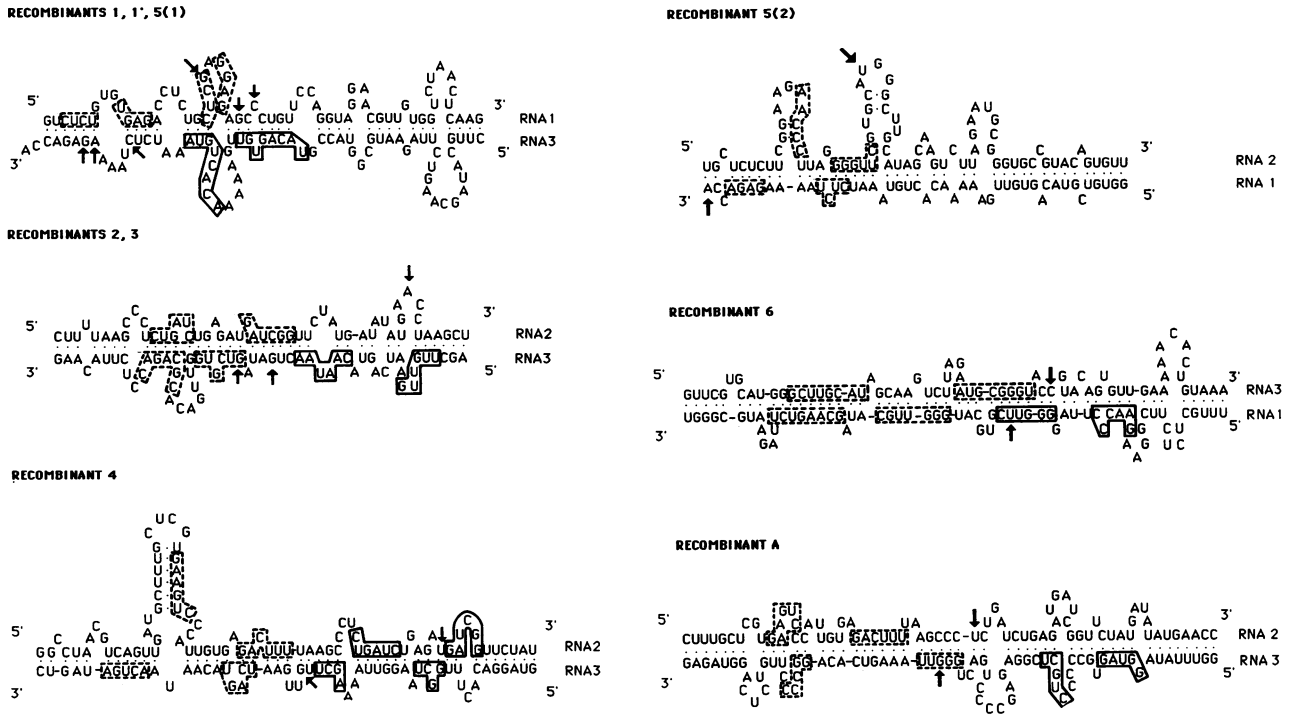


FIG. 4. Complementary sequences between pairs of positive strands of BMV RNA components (indicated on the right), as hybridized in opposite orientations near recombination sites (shown by arrows) and leading to the formation of the recombinants shown in Fig. 3. Each recombinant contains the top-strand sequences up to the arrow and then continues with the bottom-strand sequences 5′ of the bottom-strand arrow. The base-pairings are represented by dots. The numbers 5(1) and 5(2) name two different nonhomologous crossovers found in recombinant 5. Hairpin stems that can fold in putative recombination intermediates (after partial unwinding by the replicase of the hybridized duplexes) are indicated by open boxes, whereas those that may further destabilize hybridized parts of the intermediates are within dotted-line boxes. Statistical values of these alignments (in SD) and the free energies of the heteroduplexes and of the sum of intramolecular foldings for both strands (in parentheses) were as follows: recombinants 1 and 1′, 1.4 SD, −22.4 (−25.9) kcal/mol; recombinants 2 and 3, 1.9 SD, −34.1 (−20.2) kcal/mol; recombinant 4, 2.2 SD, −30.7 (−16.3) kcal/mol; recombinant 5(1), 1.5 SD, −23.8 (−33.4) kcal/mol; recombinant 5(2), 3.1 SD, −20.2 (−28.1) kcal/mol; recombinant 6, 1.7 SD, −27.0 (−40.5) kcal/mol; recombinant A, 1.7 SD, −48.3 (−28.5) kcal/mol. Free energies of the alignments were calculated according to Jacobson et al. (17), whereas those of intermolecular foldings were estimated by using the program FOLD (36).

sequenced from each progeny BMV RNA library. Among the identified 3′ recombinants shown in Fig. 3, two recombinants (variants 7 and 8) originated by homologous recombination with corresponding sequences from RNA1 and RNA2, respectively. Of seven illegitimate recombinants, variants 1 and 1′ contained 3′ end sequences of the last 236 and 235 nucleotides, respectively, from RNA1 connected at similar positions near the 3′ end of the unrepaired M4 RNA3. Recombinants 2, 3, and 4 contained almost the entire RNA2 noncoding region connected at various points in the middle of the RNA3 noncoding region. Variants 5 and 6 were derived by double crossover events. Specifically, variant 5 contained a mosaic of RNA1 and RNA2 3′ noncoding sequences joined just 12 bases upstream from the 3′ end of the M4 RNA3 molecule. RNA1 and RNA2 sequences were arranged in such a way that 75 3′-terminal nucleotides from RNA2 were ligated to the very 3′-terminal nucleotide of a 243-base-long 3′-end RNA1 sequence. In variant 6, the RNA1 insert was connected downstream to the RNA3 sequence so that it produced a 42-base deletion within the tRNA-like structure. Upstream, this RNA1 insert was legitimately ligated to RNA3 sequences. Recombinant A had the 308-base 3′ sequence from RNA2 ligated to RNA3 near the coat protein termination codon (10).

**Characterization of sequences at recombinant junctions.** To learn whether specific RNA sequences control the recombinant crosses, sequences flanking the illegitimate junctions were examined. Initial comparisons revealed no obvious similarity between primary sequences. Also, the junctions occurred between different nucleotides. This suggested that primary structures did not directly determine the recombination.

Analyzing other factors, we used the computer programs BESTFIT and GAP to investigate complementarities among the RNA substrates. Pairs of BMV RNAs comprising nucleotides from −50 to +50, both of positive polarity, were lined up in opposite orientations to form the heteroduplex structures. The best-hybridizing duplexes are shown in Fig. 4. The statistical values for these pairings, based on a mean of 25 randomized (shuffled) comparisons, ranged between 1.4 and 3.1 standard deviations (SD). A score of 3.0 SD or more is considered to demonstrate an authentic relationship (13). Therefore, at least the duplex 5(2) can be considered statistically significant. Although other heteroduplexes were statistically less probable, they may still be valid because the viruses cannot randomize their RNA sequences.

Since the number of RNA arrangements that have similar energies may be large, other configurations in the recombination regions were possible. Certainly intramolecular secondary elements may compete with the intermolecular hy-

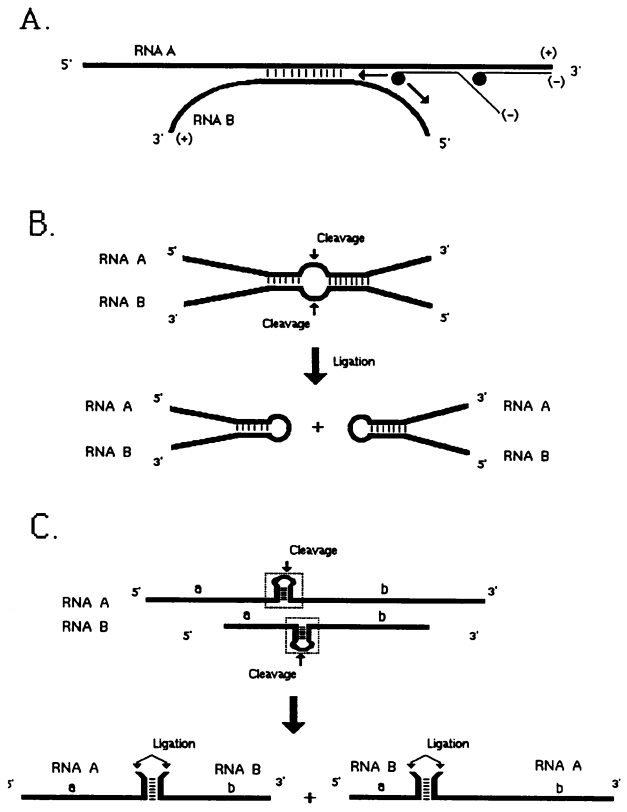


FIG. 5. Schematic illustration of the potential role of sequence complementarities in copy choice (A) and breakage-and-religation (B and C) models of recombination. (A) This continuous copy choice model involves temporary formation of a local heteroduplex between two RNAs of the same polarity. When the viral RNA polymerase reaches this region, it may continue daughter strand synthesis on the primary template A or may switch to template B. (B) In the breakage-and-religation model, two RNA molecules form a local heteroduplex structure (as in panel A) that can be cleaved within a loop region, and subsequently the already-hybridized fragments can be religated. (C) The discontinuous version of the breakage-and-religation mechanism involves separate cleavages of two viral RNAs within homologous hairpins (enclosed in the dotted open box) and a religation reaction among the two partially hybridized fragments (depicted by the lowercase letters a and b).

bridizations. To assess such a possibility, the free energies of the heteroduplexes were compared with the sum of minimal energy foldings of the corresponding ssRNA regions. As shown in the legend to Fig. 4, these values ranged within a similar order of magnitude, with some of the heteroduplex energies exceeding those for the corresponding intramolecular foldings. This indicated that hybridizations of parental BMV RNAs at the crossing sites were energetically permissible.

In addition to the hybridizations at the illegitimate junctions, associations among the accurately juxtaposed 3′ BMV RNA sequences were possible. We found that, owing to a close homology between the highly structured 3′ noncoding sequences, such interactions were more perfect and extended over longer regions than those of Fig. 4 (data not shown). The replicase switches at such duplexes may lead to the formation of the legitimate recombinants observed in this work.

## DISCUSSION

The lack of common primary sequences on both sides of the BMV recombinant crossing points is in contrast to the data of Cascone et al. (11) on recombination in TCV. Apparently, a consensus motif, similar among the terminal sequences of the genomic, satellite, and defective interfering TCV RNAs, could be located on the right sides of the TCV recombinants. Based on that, the authors proposed a replicase-driven mechanism by which the TCV RNA polymerase initiates minus-strand synthesis at either terminal or internal replicase recognition sequences. In some respects, this model is similar to the mechanism of recombination proposed for coronaviruses, in which a common leader initiates RNA synthesis at different internal sites (4).

In BMV, the heteroduplex structures at both sides of the junctions (Fig. 4) suggest that, as in poliovirus (31), local hybridizations, rather than primary sequences, may assist the RNA polymerase to switch among the BMV RNA templates (Fig. 5A). Since the detachment of the polymerase-nascent strand complex is not required in this continuous copy choice model, it should be kinetically favorable over alternative discontinuous copy choice processes. The model explains equally well the formation of both legitimate and illegitimate 3′ recombinants.

A detailed molecular mechanism for the template switchings by BMV replicase is not obvious. One common feature of the hybridizations shown in Fig. 4 is that the junctions for the downstream (donor) RNA sequences were located more towards the 3′ side than those for the upstream (acceptor) RNA sequences. This asymmetry may reflect the configuration of the putative recombination intermediates. That is, when the upcoming BMV polymerase partially unwinds the intermolecular duplex, the released parts can form intrastrand secondary elements (boxed sequences in Fig. 4). Also, the remaining duplex structures can be further shortened by folding into hairpins. All these foldings may establish a special configuration that brings the crossing sites on both RNA strands closer to each other. Moreover, it is known that the secondary-structure elements tend to weaken polymerase-RNA template interactions. Therefore, as postulated by Cascone et al. (11) and Romanova et al. (31), the upstream hairpins can detach the replicase from the primary template, thus facilitating RNA switches. The strand-separating activity of BMV replicase was shown before by demonstration of its ability to copy through partially double-stranded regions (1).

The identified illegitimate recombinants were essentially of two kinds: those resulting from crossovers between two internal 3′ noncoding portions (recombinants 2, 3, 4, 6, and A) and those resulting from crosses between an internal part of one RNA and the 3′ terminus of the second RNA (recombinants 1, 1′, and 5). The heteroduplexes in Fig. 4 explain the internal copy choice events, but they do not justify the proximal-end strand switchings. This is because the upcoming RNA polymerase would separate all of the paired region before a copy choice event could occur. Therefore, it is possible that additional mechanisms, such as a third-RNA-mediated copy choice (23) or breaking and religation (see below), may contribute to the generation of BMV recombinants.

Theoretically, the RNA recombinants may constitute at the level of either plus- or minus-strand synthesis. However, since the concentration of positive strands greatly exceeds that of negative strands, the plus strands are more likely to interact, and thus the exchanges occur during minus-strand

synthesis. Indeed, Rao and Hall (27) have demonstrated that a nonreplicating BMV RNA2 mutant recovered its replication abilities in protoplast infections. Also, we have found that a 3′-truncated (thus nonreplicating) BMV RNA3 molecule acquired its missing sequences from the wt (replicating) RNA1 or RNA2 in whole-plant infections (26a). If a copy choice mechanism operates, such a repair was possible only during minus-strand synthesis, when the RNA polymerase, upon initiation on the wt RNA1 or RNA2, could switch to the 3′-truncated input RNA3.

Breakage-and-religation mechanisms are also possible (Fig. 5). In model B, two RNA molecules form a local heteroduplex structure (as in model A), but instead of template switching by the replicase, both RNA strands are cleaved at unhybridized nucleotides and religated. Alternatively, the RNA fragments, pregenerated by cleavages at the homologous hairpin-loop structures, can be rehybridized within the complementary terminal regions and religated (model C). Since model C requires defined cleavages within the RNase-resistant 3′ noncoding regions of BMV RNAs (6), this mechanism is less probable.

## ACKNOWLEDGMENTS

We thank Paul Ahlquist for providing infectious transcribable cDNA clones of wt BMV RNA components and for communication of cowpea chlorotic mottle virus recombination results prior to publication. We are grateful to Mitchell Altschuler, Stan Flasinski, Gabriel Holbrook, Peter Nagy, Javier Romero, and Tom Zinnen for critically reading the manuscript.

This work was supported by Public Health Service grants AI26769-01A2 and BRSG S07 RR07116 (awarded by the Biomedical Research Grant Program) from the Institute of Infectious Diseases and by the Plant Molecular Biology Center at Northern Illinois University.

## REFERENCES

1. **Ahlquist, P., J. J. Bujarski, P. Kaesberg, and T. C. Hall.** 1984. Localization of the replicase recognition site within brome mosaic virus RNA by hybrid-arrested RNA synthesis. Plant Mol. Biol. **3**:37–44.
2. **Ahlquist, P., R. Dasgupta, and P. Kaesberg.** 1981. Near identity of 3′ RNA secondary structure in bromoviruses and cucumber mosaic virus. Cell **23**:183–189.
3. **Allison, R., C. Thompson, and P. Ahlquist.** 1990. Regeneration of a functional RNA virus genome by recombination between deletion mutants and requirement for cowpea chlorotic mottle virus 3a and coat genes for systemic infection. Proc. Natl. Acad. Sci. USA **87**:1820–1824.
4. **Baker, S. C., and M. M. C. Lai.** 1990. An *in vitro* system for the leader-primed transcription of coronavirus mRNAs. EMBO J. **9**:4173–4179.
5. **Banner, L. R., J. G. Keck, and M. M. C. Lai.** 1990. A clustering of RNA recombination sites adjacent to a hypervariable region of the peplomer gene of murine coronavirus. Virology **175**:548–555.
6. **Bastin, M., R. Dasgupta, T. C. Hall, and P. Kaesberg.** 1976. Similarity in structure and function of the 3′-terminal region of the four brome mosaic virus RNAs. J. Mol. Biol. **103**:737–745.
7. **Bouzoubaa, S., U. Niesbach-Klosgen, I. Jupin, H. Guilley, K. Richards, and G. Jonard.** 1991. Shortened forms of beet necrotic yellow vein virus RNA-3 and -4: internal deletions and subgenomic RNA. J. Gen. Virol. **72**:259–266.
8. **Bujarski, J. J., P. Ahlquist, T. C. Hall, T. W. Dreher, and P. Kaesberg.** 1986. Modulation of replication, aminoacylation and adenylation *in vitro* and infectivity *in vivo* of BMV RNAs containing deletions within the multifunctional 3′ end. EMBO J. **5**:1769–1774.
9. **Bujarski, J. J., T. W. Dreher, and T. C. Hall.** 1985. Deletions in the 3′-terminal tRNA-like structure of brome mosaic virus RNA differentially affect aminoacylation and replication *in vitro*. Proc. Natl. Acad. Sci. USA **82**:5636–5640.
10. **Bujarski, J. J., and P. Kaesberg.** 1986. Genetic recombination in a multipartite plant virus. Nature (London) **321**:528–531.
11. **Cascone, P. J., C. D. Carpenter, X. H. Li, and A. Simon.** 1990. Recombination between satellite RNAs of turnip crinkle virus. EMBO J. **9**:1709–1715.
12. **Dawson, W. O., D. J. Lewandowski, M. E. Hilf, P. Bubrick, A. J. Raffo, J. J. Shaw, G. L. Grantham, and P. R. Desjardins.** 1989. A tobacco mosaic virus-hybrid expresses and loses an added gene. Virology **172**:285–292.
13. **Doolittle, R. F.** 1981. Similar amino acid sequences: chance or common ancestry? Science **214**:149–159.
14. **Fields, S., and G. Winter.** 1982. Nucleotide sequences of influenza virus segments 1 and 3 reveal mosaic structure of a small viral RNA segment. Cell **28**:303–313.
15. **Hillman, B. I., J. C. Carrington, and T. J. Morris.** 1987. A defective interfering RNA that contains a mosaic of a plant virus genome. Cell **51**:427–433.
16. **Huisman, M. J., B. J. C. Cornelissen, C. F. M. Groenendijk, J. F. Bol, and L. van Vloten-Doting.** 1989. Alfalfa mosaic virus temperature-sensitive mutants. V. The nucleotide sequence of TBS 7 RNA 3 shows limited nucleotide changes and evidence for heterologous recombination. Virology **171**:409–416.
17. **Jacobson, A. B., L. Good, J. Simonetti, and M. Zuker.** 1984. Some simple computational methods to improve the folding of large RNAs. Nucleic Acids Res. **12**:45–52.
18. **Janda, M., R. French, and P. Ahlquist.** 1987. High efficiency T7 polymerase synthesis of infectious RNA from cloned brome mosaic virus cDNA and effects of 5′ extensions of transcript infectivity. Virology **158**:259–262.
19. **Keck, J. G., S. A. Stohlman, S. Soe, S. Makino, and M. M. C. Lai.** 1987. Multiple recombination sites at the 5′ end of murine coronavirus RNA. Virology **156**:331–334.
20. **King, A. M. Q.** 1988. Genetic recombination in positive strand RNA viruses, p. 149–165. *In* E. Domingo, J. J. Holland, and P. Ahlquist (ed.), RNA genetics, vol. 2. CRC Press, Boca Raton, Fla.
21. **King, A. M. Q., D. McCahon, W. R. Slade, and J. W. I. Newman.** 1982. Recombination in RNA. Cell **29**:921–928.
22. **Kirkegaard, K., and D. Baltimore.** 1986. The mechanism of RNA recombination in poliovirus. Cell **47**:433–443.
23. **Kuge, S., N. Kawamura, and A. Nomoto.** 1989. Genetic variation occurring on the genome of an in vitro insertion mutant of poliovirus type 1. J. Virol. **63**:1069–1075.
24. **Lane, L.** 1986. Propagation and purification of RNA plant viruses. Methods Enzymol. **118**:687–696.
25. **McCahon, D., A. M. Q. King, D. S. Roe, W. R. Slade, and J. W. I. Newman.** 1985. Isolation and biochemical characterization of intertypic recombinants of foot-and-mouth disease virus. Virus Res. **3**:87–100.
26. **Miller, W. A., J. J. Bujarski, T. W. Dreher, and T. C. Hall.** 1986. Minus strand initiation by brome mosaic virus replicase within the 3′ tRNA-like structure of native and modified RNA templates. J. Mol. Biol. **187**:537–546.

26a. **Nagy, P., and J. Bujarski.** Unpublished data.

27. **Rao, A. L. N., and T. C. Hall.** 1990. Requirement for a viral *trans*-acting factor encoded by brome mosaic virus RNA-2 provides strong selection in vivo for functional recombinants. J. Virol. **64**:2437–2441.
28. **Rao, A. L. N., B. P. Sullivan, and T. C. Hall.** 1990. Use of *Chenopodium hybridum* facilitates isolation of brome mosaic virus RNA recombinants. J. Gen. Virol. **71**:1403–1407.
29. **Rietveld, K., C. W. A. Pleij, and L. Bosch.** 1983. Three-dimensional models of the tRNA-like 3′ termini of some plant viral RNAs. EMBO J. **2**:1079–1085.
30. **Robinson, D. J., W. D. O. Hamilton, B. D. Harrison, and D. C. Baulcombe.** 1987. Two anomalous tobravirus isolates: evidence for RNA recombination in nature. J. Gen. Virol. **68**:2551–2561.
31. **Romanova, L. I., V. M. Blinov, E. A. Tolskaya, E. G. Viktorova, M. S. Kolesnikowa, E. A. Guseva, and V. I. Agol.** 1986. The primary structure of crossover regions of intertypic poliovirus recombinants: a model of recombination between RNA genomes. Virology **155**:202–213.

32. **Sambrook, J., E. F. Fritsch, and T. Maniatis.** 1989. Molecular cloning: a laboratory manual, 2nd ed. Cold Spring Harbor Laboratory, Cold Spring Harbor, N.Y.
33. **Shirako, Y., and M. K. Brakke.** 1984. Spontaneous deletion mutation of soil-borne wheat mosaic virus. II. J. Gen. Virol. **65**:855–858.
34. **Smith, D. B., and S. C. Inglis.** 1987. The mutation rate and variability of eucaryotic viruses: an analytical review. J. Gen. Virol. **68**:2729–2740.
35. **Tolskaya, E. A., L. A. Romanova, V. M. Blinow, E. G. Viktorova, A. N. Sinyakov, M. S. Kolesnikova, and V. I. Agol.** 1988. Studies on the recombination between RNA genomes of poliovirus: the primary structure and nonrandom distribution of crossover regions in the genomes of intertypic poliovirus recombinants. Virology **161**:54–61.
36. **Zucker, M., and P. Stiegler.** 1981. Optimal computer folding of large RNA sequences using thermodynamics and auxiliary information. Nucleic Acids Res. **9**:133–148.